Universität des Saarlandes

Fachrichtung 6.1 – Mathematik

Preprint Nr. 322

A New Fundamental Solution Method Based on the Adaptive Cross Approximation

Marvin Fleck, Richards Grzhibovskis and Sergej Rjasanow

Saarbrücken 2012

Fachrichtung 6.1 – Mathematik
Universität des Saarlandes

Preprint No. 322
submitted: January 11, 2013

A New Fundamental Solution Method Based on the Adaptive Cross Approximation

Marvin Fleck
Saarland University
Department of Mathematics
P.O. Box 15 11 50
66041 Saarbrücken
Germany
fleck@num.uni-sb.de

Richards Grzhibovskis
Saarland University
Department of Mathematics
P.O. Box 15 11 50
66041 Saarbrücken
Germany
richards@num.uni-sb.de

Sergej Rjasanow
Saarland University
Department of Mathematics
P.O. Box 15 11 50
66041 Saarbrücken
Germany
rjasanow@num.uni-sb.de

Edited by
FR 6.1 – Mathematik
Universität des Saarlandes
Postfach 15 11 50
66041 Saarbrücken
Germany

Fax: + 49 681 302 4443
e-Mail: preprint@math.uni-sb.de
WWW: http://www.math.uni-sb.de/

A New Fundamental Solution Method Based on the Adaptive Cross Approximation

M. Fleck, R. Grzhibovskis, S. Rjasanow

January 11, 2013

Abstract

A new adaptive Fundamental Solution Method (FSM) for the approximate solution of scalar elliptic boundary value problems is presented. The construction of the basis functions is based on the Adaptive Cross Approximation (ACA) of the fundamental solution of the corresponding elliptic operator. An algorithm for an immediate computer implementation of the method is formulated. A series of numerical examples for the Laplace and Helmhotz equations in three dimensions illustrates the efficiency of the method. Extensions of the method to elliptic systems are discussed.

1 Introduction

The Fundamental Solution Method (FSM) is also known as the Method of Fundamental Solutions, Charge Simulation Method or as a special version of the Boundary Collocation Method. It resembles a Trefftz method [7], which means that the solution to a Dirichlet boundary value problem in $\Omega \subset \mathbb{R}^3$, $\Gamma = \partial\Omega$

$$\mathcal{L}u(x) = 0\,, \quad \text{for } x \in \Omega\,, \tag{1}$$

$$u(x) = g(x)\,, \quad \text{for } x \in \Gamma\,, \tag{2}$$

is approximated by a linear combination of $\mathcal{L}$-harmonic functions. As the name indicates the method uses fundamental solutions for basis functions, whose singularities are located outside Ω. It was introduced by Kupradze and Aleksidze [4] in 1963 for treating the Laplace equation. First investigations from a numerical point of view were performed by Mathon and Johnston [5] in 1977. Comprehensive summaries of the attributes of the FSM were written, among others, by Smyrlis [6] and Bogomolny [3].

Two peculiar aspects of the Fundamental Solution Method are an extremely fast convergence, but also a very high condition number of the system matrix, both

with respect to the number of collocation points. We adress the problem of high condition numbers by adaptively choosing a smaller number of collocation points while keeping the local error below a given threshold, but not neccessarily equal to zero, for the remaining collocation points. Thus an approximation is obtained, while condition numbers are kept lower due to smaller system matrices. The quality of the approximation is comparable to that of classical FSM. By means of this approach problems that are to big for classical FSM can be treated. The adaptive strategy features new basis functions, which vanish in collocation points already treated and thus do not alter the corresponding local approximation. The construction of these basis functions uses concepts from the Adaptive Cross Approximation (ACA) [2].
In Section 2 we formulate a model problem and present the classical (collocation-based) Fundamental Solution Method. Section 3 briefly summarizes the Adaptive Cross Approximation. The approximation algorithm presented therein leads directly to the construction of basis functions for the Adaptive Fundamental Solution Method in Section 4. In Section 5 we present numerical results for the adaptive method applied to the Laplace and Helmholtz equations respectively.

2 Formulation of the problem

We consider the following Dirichlet boundary value problem for an elliptic equation in $\mathbb{R}^3$

$$\begin{aligned} \mathcal{L}u(x) &= 0\,, \quad \text{for } x \in \Omega\,, && \text{(3a)} \\ u(x) &= g(x)\,, \quad \text{for } x \in \Gamma\,, && \text{(3b)} \end{aligned}$$

where $\mathcal{L}$ is an elliptic differential operator of the second order and $\Omega \subset \mathbb{R}^3$ is a Lipschitz domain with the boundary Γ. In the classical setting, the Dirichlet datum g is assumed to be continuous on Γ and the solution u is assumed to be smooth, i.e.

$$u \in C^2(\Omega) \cap C(\overline{\Omega})\,. \tag{4}$$

In this paper, we will consider the Laplace operator

$$\mathcal{L}u = -\Delta u \tag{5}$$

and the Helmholtz operator

$$\mathcal{L}u = -\Delta u - \kappa^2 u\,. \tag{6}$$

For these operators the corresponding fundamental solution u^*, i.e. the solution of the equation

$$\mathcal{L}u^* = \delta \tag{7}$$

in the distributional sense, is known and given by

$$u^*(x) = \frac{1}{4\pi}\,\frac{1}{|x|} \tag{8}$$

for the Laplace operator, and

$$u^*(x) = \frac{1}{4\pi}\,\frac{e^{\imath\kappa|x|}}{|x|} \tag{9}$$

for the Helmholtz operator. In (7) δ denotes the Dirac δ-distribution.

2.1 Fundamental solution method

Let $X \subset \Gamma$ be a discrete set of N pairwise different control (collocation) points on the boundary Γ and $Y \subset \mathbb{R}^3 \setminus \overline{\Omega}$ a discrete set of N pairwise different singularity points. Consider a system of basis functions

$$\Phi = \left\{\varphi_1, \ldots, \varphi_N\right\},\ \varphi_\ell(x) = u^*(x - y_\ell)\,,\ y_\ell \in Y\,,\ \ell = 1, \ldots, N\,. \tag{10}$$

Since $y_\ell \notin \overline{\Omega}\,,\ \ell = 1, \ldots, N$, every basis function φ_ℓ is $\mathcal{L}$-harmonic in Ω and the function

$$u_N(x) = \sum_{\ell=1}^{N} \alpha_\ell \varphi_\ell(x) = \Phi(x)\underline{a}\,, \quad \underline{a} = (\alpha_1, \ldots, \alpha_N)^\top \in \mathbb{R}^N \tag{11}$$

can be considered as an approximation of the solution u of the boundary value problem (3). The most simple choice for the coefficients α_ℓ is the point collocation for the boundary condition:

$$u_N(x) = g(x)\,, \quad \text{for } x \in X\,. \tag{12}$$

This can be equivalently formulated as a linear system for obtaining N coefficients α_l:

$$\sum_{\ell=1}^{N} \alpha_\ell \varphi_\ell(x_k) = g(x_k)\,, \quad \text{for } k = 1, \ldots, N \tag{13}$$

or

$$F\underline{a} = \underline{g}\,, \quad F = \Big(\varphi_\ell(x_k)\Big)_{k,\ell=1}^{N} \in \mathbb{R}^{N\times N}\,, \quad \underline{a}, \underline{g} \in \mathbb{R}^N\,. \tag{14}$$

The main properties of the FSM can be summarised as follows.

1. Since no topology of the discrete point sets X and Y is required, the FSM can be considered as a meshfree numerical method.

2. The entries of the matrix F in (14) are easy to compute as opposed to matrix entries coming from Boundary Element Methods (BEM).

3. The dimension of the matrix F is comparable to those of the BEM (e.g. $N \sim 10^4 - 10^5$ for 3D problems).

4. The matrix F is fully populated as in the BEM and $Mem(F) = \mathcal{O}(N^2)$.

5. The condition number of the matrix F grows exponentially, i.e. $\mathrm{cond}(F) = \mathcal{O}(q^N)$ for some $q > 1$.

For large N the application of a direct solver to the system (14) is expensive, while an iterative solver does not converge due to the extremely high condition number of the matrix F.
However, for analytic boundary data the numerical results for small systems show an exponential convergence of the method not only for the solution u itself but also for its gradient

$$\mathrm{grad} u = \left(\frac{\partial u}{\partial x_1}, \frac{\partial u}{\partial x_2}, \frac{\partial u}{\partial x_3} \right)^\top$$

and even for its Hessian matrix

$$\mathcal{H}u = \left(\frac{\partial^2 u}{\partial x_k \partial x_\ell} \right)_{k,\ell=1}^{3},$$

i.e.

$$\begin{aligned} \mathcal{O}(|u(x) - u_N(x)|) &= \mathcal{O}(\big|\mathrm{grad}\big(u(x) - u_N(x)\big)\big|) \\ &= \mathcal{O}(\big|\big|\mathcal{H}\big(u(x) - u_N(x)\big)\big|\big|_F) \\ &= \mathcal{O}(q^{-N}) \end{aligned}$$

for $x \in \Omega$. Note that the derivatives of the approximate solution u_N can be easily computed analytically.
In fact the rate of convergence depends on the smoothness of the boundary data. A known result for two-dimensional problems on annular domains or domains whose boundaries are analytic Jordan curves is that for $C^l(\Gamma)$-data the error is $\mathcal{O}(N^{1-l})$ [6]. Numerical experiments confirm that the method has difficulties with nonsmooth boundary data.

2.2 Choice of Pseudo Boundary

In the theoretical analysis of Fundamental Solution Methods one introduces the concept of pseudo boundaries, i.e. surfaces where the singularity points are located. Pseudo boundaries fulfilling the so-called embracing condition provide for the suitability of corresponding fundamental solutions as basis functions [6].

However, one still has great freedom of choice of an actual pseudo boundary and in the subsequent choice of the location of singularity points.
We briefly present the definition and central theorem for pseudo boundaries. A thorough overview can be found in [6].

Definition 1 (Segment condition)**.** *Let $\Omega \subset \mathbb{R}^d$ be an open set. Ω fulfills the segment condition, if for every $x \in \partial\Omega$ there exists a neighbourhood $U(x)$ of x and a nonzero vector $\xi(x) \in \mathbb{R}^d$, such that, if $y \in U(x) \cap \bar{\Omega}$, then $y + t\xi(x) \in \Omega,\ \forall t \in (0,1)$.*

Definition 2 (Embracing boundary)**.** *Let $\Omega, \Omega' \subset \mathbb{R}^d$ open and connected. Ω' embraces Ω, if:*

1. *$\bar{\Omega} \subset \Omega'$*
2. *For each connected component V of $\mathbb{R}^d \setminus \bar{\Omega}$ there is an open connected component V' of $\mathbb{R}^d \setminus \bar{\Omega}'$, such that $\bar{V}' \subset V$.*

Theorem 1. *If $\Omega \subset \mathbb{R}^d$ fulfills the segment condition and $\Omega' \subset \mathbb{R}^d$ embraces Ω, then for $d \geq 3$ and $l \geq 0$ the space $\mathcal{X}$ spanned by finite linear combinations of Fundamental solutions*

$$u_N(x) = \sum_{j=1}^{N} \alpha_j u^*(x - y_j)$$

with singularities $y_j \in \partial\Omega'$ is dense in

$$\mathcal{Y}_l = \{v \in C^2(\Omega) : \Delta v = 0 \text{ in } \Omega\} \cap C^l(\bar{\Omega})$$

with respect to the norm of $C^l(\bar{\Omega})$. For $d = 2$ the density result holds true for $\mathcal{X} \oplus \{c \cdot 1|_{\bar{\Omega}} : c \in \mathbb{R}\}$.

Proof. The proof can be found in [6]. □

Similar results exist for operators Δ^m, $m > 1$, and $\Delta - \kappa^2$, $\kappa > 0$, [6, 3].
One can proof in the two-dimensional case that an increase in the distance between the boundary $\partial\Omega$ and the pseudo boundary $\partial\Omega'$ leads to both, better approximation and larger condition number of F. This is also observed in three-dimensional settings.
For simple domain shapes the common choice of the singularity points consists in shifting collocation points along the outer normal. This strategy may fail for more complex domains. On the other hand the construction of pseudo boundaries by means of distance functions can be computationally expensive.
In what follows we will introduce a new method with the same convergence properties but almost without disadvantages of the FSM, i.e. without necessity of the numerical solving of big, dense and badly conditioned systems of linear equations. Our main tool is the Adaptive Cross Approximation.

3 Adaptive Cross Approximation

The initial analytical form of the ACA algorithm was designed to interpolate and, hopefully, to approximate a given function $K : \mathbb{X} \times \mathbb{Y} \to \mathbb{R}$ of two variables x and y by a degenerate function S_n, i.e.

$$K(x, y) \approx S_n = \sum_{\ell=1}^{n} u_\ell(x) v_\ell(y) \,, \tag{15}$$

where $u_l : \mathbb{X} \to \mathbb{R}$, $v_l : \mathbb{Y} \to \mathbb{R}$, $l = 1, \ldots, n$. The construction is as follows. Let $X \subset \mathbb{X} \subset \mathbb{R}^3$ and $Y \subset \mathbb{Y} \subset \mathbb{R}^3$ be discrete point sets.

Algorithm 1.

1. `initialization`

   `1.1 set initial residual and initial approximation`

   $$R_0(x, y) = K(x, y) \,, \quad S_0(x, y) = 0$$

   `1.2 choose initial pivot position`

   $$x_0 \in X \,, \;\; y_0 \in Y \,, \;\; R_0(x_0, y_0) \neq 0$$

2. `recursion for` $k = 0, 1, \ldots$

   `2.1 new residual`

   $$R_{k+1}(x, y) = R_k(x, y) - \frac{R_k(x, y_k) R_k(x_k, y)}{R_k(x_k, y_k)}$$

   `2.2 new approximation`

   $$S_{k+1}(x, y) = S_k(x, y) + \frac{R_k(x, y_k) R_k(x_k, y)}{R_k(x_k, y_k)}$$

   `2.3 new pivot position`

   $$x_{k+1} \in X \,, \;\; y_{k+1} \in Y \,, \;\; R_{k+1}(x_{k+1}, y_{k+1}) \neq 0$$

After $n \geq 1$ steps of the ACA-Algorithm 1, we obtain a sequence of residuals $R_0, \ldots, R_n$ and a sequence of approximations $S_0, \ldots, S_n$ with the following properties.

1. Approximation property for $k = 0, \ldots, n$

   $$R_k(x, y) + S_k(x, y) = K(x, y) \,, \;\; x \in X \,, y \in Y \tag{16}$$

2. Interpolation property for $k = 1, \ldots, n$ and $\ell = 0, \ldots, k-1$

$$R_k(x, y_\ell) = R_k(x_\ell, y) = 0\,,\ x \in X\,, y \in Y \tag{17}$$

or

$$S_k(x, y_\ell) = K(x, y_\ell)\,,\ x \in X\,, \quad S_k(x_\ell, y) = K(x_\ell, y)\,,\ y \in Y \tag{18}$$

3. Harmonicity property for $k = 0, \ldots, n$
If

$$\mathcal{L}_x K(x, y) = 0\,,\ x \in \Omega$$

then

$$\mathcal{L}_x R_k(x, y) = \mathcal{L}_x S_k(x, y) = 0\,,\ x \in \Omega$$

4. Non-recursive representation for $k = 1, \ldots, n$

$$S_k(x, y) = u_k^\top(x) V_k^{-1} w_k(y)\,,\ V_k \in \mathbb{R}^{k\times k}\,,\ u_k(x), w_k(y) \in \mathbb{R}^k \tag{19}$$

with

$$u_k(x) = \big(K(x, y_0), \ldots, K(x, y_{k-1})\big)^\top\,,$$
$$w_k(y) = \big(K(x_0, y), \ldots, K(x_{k-1}, y)\big)^\top$$

and

$$V_k = \Big(K(x_i, y_j)\Big)_{i,j=0}^{k-1}$$

The above properties, except the last one, can be easily seen. The proof of the non-recursive representation is more technical and can be found in [2].

4 Adaptive FSM

In this section, we formulate a new adaptive FSM for the boundary value problem (3). Let u^* be the fundamental solution of the differential operator $\mathcal{L}$, $X \subset \Gamma$ a discrete set of the control points, $Y \subset \mathbb{R}^3 \setminus \overline{\Omega}$ a discrete set of the singularity points and ε an upper threshold for the error in the collocation points.

Algorithm 2.

1. `initialization`

   `1.1 initial error and initial pivot position`

$$Error_1 = \texttt{Max}_{x\in X}|g(x)|\,, \quad x_1 = \texttt{ArgMax}_{x\in X}|g(x)|$$

1.2 initial residual

$$R_1(x,y) = u^*(x-y)\,,$$

1.3 first basis function

$$\varphi_1(x) = \frac{R_1(x,y_1)}{R_1(x_1,y_1)}$$

1.4 first approximation

$$u_1(x) = \alpha_1\varphi_1(x)\,, \quad \alpha_1 = g(x_1)$$

2. recursion for $k = 1, 2, \ldots$

2.1 new error and new pivot position

$$Error_{k+1} = \mathtt{Max}_{x\in X}|g(x) - u_k(x)|\,, \quad x_{k+1} = \mathtt{ArgMax}_{x\in X}|g(x) - u_k(x)|$$

2.2 stopping criteria
Stop if $Error_{k+1} \le \varepsilon$ or $k = \#$ of points in X

2.3 next residual

$$R_{k+1}(x,y) = R_k(x,y) - \frac{R_k(x,y_k)R_k(x_k,y)}{R_k(x_k,y_k)} \tag{20}$$

2.4 next basis function

$$\varphi_{k+1}(x) = \frac{R_{k+1}(x,y_{k+1})}{R_{k+1}(x_{k+1},y_{k+1})} \tag{21}$$

2.5 next approximation

$$u_{k+1}(x) = u_k(x) + \alpha_{k+1}\varphi_{k+1}(x)\,, \quad \alpha_{k+1} = g(x_{k+1}) - u_k(x_{k+1})$$

After n steps of the above algorithm, an approximation

$$u_n(x) = \sum_{k=1}^{n} \alpha_k\varphi_k(x) \tag{22}$$

is obtained. The basis functions φ_k are $\mathcal{L}$-harmonic for all $k = 1, \ldots, n$

$$\mathcal{L}\varphi_k(x) = 0\,, \quad \text{for } x \in \Omega\,. \tag{23}$$

Therefore, also the function u_n is $\mathcal{L}$-harmonic

$$\mathcal{L}u_n(x) = 0\,, \quad \text{for } x \in \Omega\,. \tag{24}$$

The function u_n fulfills the boundary condition pointwise in the pivot points

$$u_n(x_k) = g(x_k)\,, \quad \text{for } k = 1, \ldots, n \tag{25}$$

and approximates the boundary condition in other points

$$\big|u_n(x) - g(x)\big| \leq \varepsilon\,, \quad \text{for } x \in X \setminus \big\{x_1, \ldots, x_n\big\}\,. \tag{26}$$

Later on, our numerical examples will show that the number n of steps required to obtain a given accuracy is rather small compared to, and seems to be independent of, the number of control points N, i.e. $n \ll N$. Due to the ACA interpolation property of the residuals R_k, the basis functions $\varphi_k\,,\ k \geq 2$ vanish on all previous pivot points

$$\varphi_k(x_\ell) = 0\,,\ \ell = 1, \ldots, k-1\,,\ k = 2, \ldots, n \tag{27}$$

and due to construction

$$\varphi_k(x_k) = 1\,,\ k = 1, \ldots, n\,. \tag{28}$$

Thus, the coefficients α_k in (22) can be easily computed as in `Step 2.5` of the Algorithm 2 without the need to solve a system of equations, or more precisely by solving small system

$$F\underline{a} = \underline{g}\,, \quad F = \Big(\varphi_\ell(x_k)\Big)_{k,\ell=1}^{n} \in \mathbb{R}^{n\times n}\,, \quad \underline{a}, \underline{g} \in \mathbb{R}^n \tag{29}$$

with the following triangular matrix

$$F = \begin{pmatrix} 1 & 0 & 0 & \ldots & 0 \\ \varphi_1(x_2) & 1 & 0 & \ldots & 0 \\ \ldots & \ldots & \ldots & \ldots & \ldots \\ \varphi_1(x_n) & \varphi_2(x_n) & \varphi_3(x_n) & \ldots & 1 \end{pmatrix}\,.$$

However, the price for the above simple and efficient algorithm is more complicated evaluation of the basis functions φ_k and, therefore, also of the approximation u_n in a given point $x \in \Omega$. We use the non-recursive representation (19) of the ACA approximation S_n, the approximation property (16), and the definition of the basis function in `Step 2.4` of the Algorithm 2 to obtain

$$\varphi_1(x) = \frac{u^*(x - y_1)}{u^*(x_1 - y_1)} \tag{30}$$

and for $k = 2, \ldots, n$

$$\varphi_k(x) = \frac{u^*(x - y_k) - u_k^\top(x) z_k}{u^*(x_k - y_k) - u_k^\top(x_k) z_k} \tag{31}$$

with

$$\begin{aligned} u_k(x) &= \big(u^*(x-y_1),\dots,u^*(x-y_{k-1})\big)^\top, \\ z_k &= V_k^{-1} w_k(y_k)\,, \\ w_k(y_k) &= \big(u^*(x_1-y_k),\dots,u^*(x_{k-1}-y_k)\big)^\top \end{aligned} \tag{32}$$

and

$$V_k = \Big(u^*(x_i-y_j)\Big)_{i,j=1}^{k-1}.$$

The vectors $z_k \in \mathbb{R}^{k-1}$ as well as the normalising constants $\big(u^*(x_1-y_1)\big)^{-1}$ and $\big(u^*(x_k-y_k) - u_k^\top(x_k) z_k\big)^{-1}$ can be precomputed during the algortihm as follows. Let

$$V_2 = L_2 U_2 = 1 \cdot u^*(x_1-y_1) \tag{33}$$

be the LU-decomposition of the 1×1-matrix V_2. Then, making use of the LU-decomposition of the $(k-1)\times(k-1)$-matrix

$$V_k = L_k U_k\,,\ k = 2,\dots,n-1\,,$$

we get for the $k\times k$-matrix V_{k+1}

$$V_{k+1} = \begin{pmatrix} L_k & 0 \\ a^\top & 1 \end{pmatrix} \begin{pmatrix} U_k & b \\ 0 & c \end{pmatrix} \tag{34}$$

with

$$L_k b = w_k(y_k)\,,\ a^\top U_k = u_k^\top(x_k)\,,\ c = u^*(x_k-y_k) - a^\top b\,. \tag{35}$$

For the vectors z_k, we get

$$z_k = U_k^{-1} L_k^{-1} w_k(y_k) = U_k^{-1} b\,. \tag{36}$$

From equations (20) and (21) we see

$$\begin{aligned} R_{k+1}(x,y) &= R_k(x,y) - R_k(x_k,y) R_k^{-1}(x_k,y_k) R_k(x,y_k) \\ &= R_k(x,y) - R_k(x_k,y)\varphi_k(x) \\ &= u^*(x-y) - \sum_{j=1}^{k} R_j(x_j,y)\varphi_j(x) \quad \forall k>0 \end{aligned}$$

and thus

$$u^*(x-y) = R_{k+1}(x,y) + \sum_{l=1}^{k} R_l(x_l,y)\varphi_l(x) \quad \forall k \geq 0. \tag{37}$$

This leads to

$$\begin{pmatrix} u^*(x_1-y_1) & \cdots & u^*(x_1-y_k) \\ \vdots & \ddots & \vdots \\ u^*(x_k-y_1) & \cdots & u^*(x_k-y_k) \end{pmatrix}$$
$$= \begin{pmatrix} 1 & 0 & \cdots & 0 \\ \varphi_1(x_2) & 1 & \cdots & 0 \\ \cdots & \cdots & \cdots & \cdots \\ \varphi_1(x_k) & \varphi_2(x_k) & \cdots & 1 \end{pmatrix} \begin{pmatrix} R_1(x_1,y_1) & R_1(x_1,y_2) & \cdots & R_1(x_1,y_k) \\ 0 & R_2(x_2,y_2) & \cdots & R_2(x_2,y_k) \\ \cdots & \cdots & \cdots & \cdots \\ 0 & 0 & \cdots & R_k(x_k,y_k) \end{pmatrix}.$$

Due to the uniqueness of the LU decomposition with unit diagonal entries we see that

$$L_n = F.$$

A numerical evaluation of the basis function φ_k in (31) requires the scalar product $u_k^\top(x)z_k$ and, therefore $\mathcal{O}(k)$ arithmetical operations. The approximate solution u_n will require $\mathcal{O}(n^2)$ artithmetical operations for every evaluation.
The adaptive Fundamental Solution Method also allows for alternative strategies for choosing the singularity points y_i. Instead of introducing fixed pairs (x_i, y_i) of collocation and singularity points we may equip a simply shaped pseudo boundary, e.g. an ellipsoid, with a large number of uniformly distributed candidate points. The adaptive FSM can be tuned to pick from those candidates the singularity point that maximizes the current basis function's pivot element $R_{k+1}(x_{k+1}, y)$ in (21).

5 Numerical examples

In order to investigate the features of the adaptive Fundamental Solution Method, we perform numerical experiments for the BVP (3) with Laplace or Helmholtz operators. We compare results of classical FSM, adaptive FSM with given thresholds as well as a threshold-free adaptive method. For the latter method we store the maximal local error of an iteration step and terminate, if no improvement is achieved after a given number of further iterations. By dropping the coefficients associated with these additional steps the currently best result (with respect to local errors) is restored.
Indicated condition numbers are calculated using LAPACK routines [1]. Condition number of respective system matrices are labeled cond_{sys}, while those of matrices required for basis function evaluation in the adaptive method are labeled cond_{LU}. In the latter case we only indicate condition numbers of the respective largest matrix, i.e. the matrix used in the evaluation of the basis function with highest index.

threshold	$e_{\max}$	e	cond_{sys}	cond_{LU}	# nodes
classical	$8.80 \cdot 10^{-10}$	$1.01 \cdot 10^{-11}$	$1.42 \cdot 10^{21}$	-	5120
10^{-4}	$9.78 \cdot 10^{-5}$	$1.08 \cdot 10^{-6}$	$1.91 \cdot 10^{2}$	$4.53 \cdot 10^{10}$	415
10^{-6}	$1.01 \cdot 10^{-6}$	$1.10 \cdot 10^{-8}$	$3.26 \cdot 10^{2}$	$8.00 \cdot 10^{12}$	711
10^{-8}	$1.05 \cdot 10^{-8}$	$1.13 \cdot 10^{-10}$	$4.94 \cdot 10^{2}$	$7.26 \cdot 10^{14}$	1069
10^{-10}	$1.09 \cdot 10^{-10}$	$1.11 \cdot 10^{-12}$	$6.09 \cdot 10^{2}$	$9.81 \cdot 10^{16}$	1531

Table 1: Laplace equation on the unit ball, $N = 5120$.

In the result tables relative errors e are presented in $L^2(\Gamma)$-norm evaluated by numerical integration. In addition the maximum of the error in the used Gauss points $e_{\max}$ is indicated.

5.1 Laplace equation

We consider the model problem

$$-\Delta v(x) = 0\,, \quad \text{for } x \in \Omega\,, \tag{38}$$

$$v(x) = g(x)\,, \quad \text{for } x \in \partial\Omega\,, \tag{39}$$

with the known analytical solution

$$v(x) = \sin(2\pi x_1) x_2 e^{-2\pi x_3}\,, \quad g = v|_\Gamma,$$

in order to display some general observations regarding the adaptive FSM, which are also relevant for other equation types we have considered. In our experiments Ω is chosen as the unit ball, a brick-shaped domain or a crankshaft-shaped domain. Singularity points are obtained by shifting collocation points by 1 along the surface normal, or in case of the crankshaft domain placed on an ellipsoidal pseudo boundary matched to the domain's shape and scaled by a factor of 1.1.

Performance of the adaptive FSM

As one can see in Table 1 the adaptive method uses only a small number of collocation points, which increases when a lower threshold is set. Even the accuracy of the full FSM can be reached with a relatively small subset of collocation points. This reduction leads to condition numbers of the involved matrices, which are significantly lower than those of the full method's system matrix. Since the approximation space of the adaptive method is always a subset of the full FSM approximation space, the outperformance in the last row of the table can only be explained by a loss of accuracy due to high condition numbers.

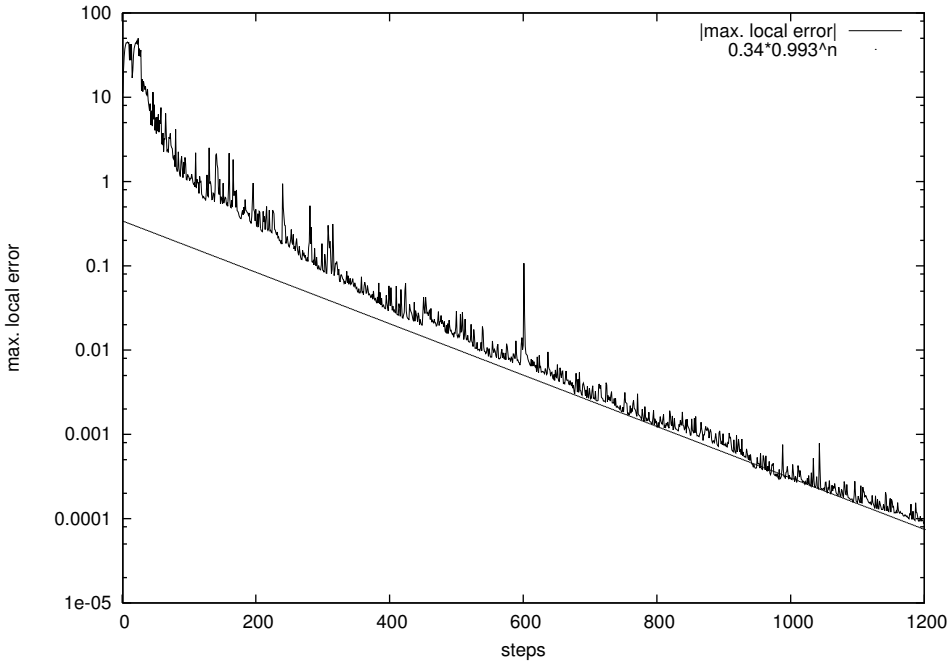

Figure 1: Evolution of maximal local error for a Laplace equation on a brick-shaped domain.

Evolution of maximal local error

The strategy of the adaptive method consists in eliminating the currently largest error of all collocation points, while not altering those in collocation points already treated. However, there is no guarantee that after any elimination step the new maximal error is actually smaller than the previous one. In fact, while the maximal error assymptotically decreases during the elimination process, short-term increases are rather typical (cf. Figure 1 for a brick-shaped domain).
For tight thresholds the adaptive method uses a number of collocation points compareable to that of classical FSM. For very large problems this may lead to errors in the evaluation of basis functions (evaluation of z_k in (32)) and ultimately to an assymptotic increase of the maximal local error. For these cases it is handy to store information about the "best" step so far and restore the corresponding result. Thus, although the threshold is not met, in these extreme cases results are far better than those of the classical method.

Distribution of errors

Both methods, classical as well as adaptive FSM, control errors in the collocation points only. Therefore the question arises, how errors behave inside the domain as well as on the boundary between the collocation points.

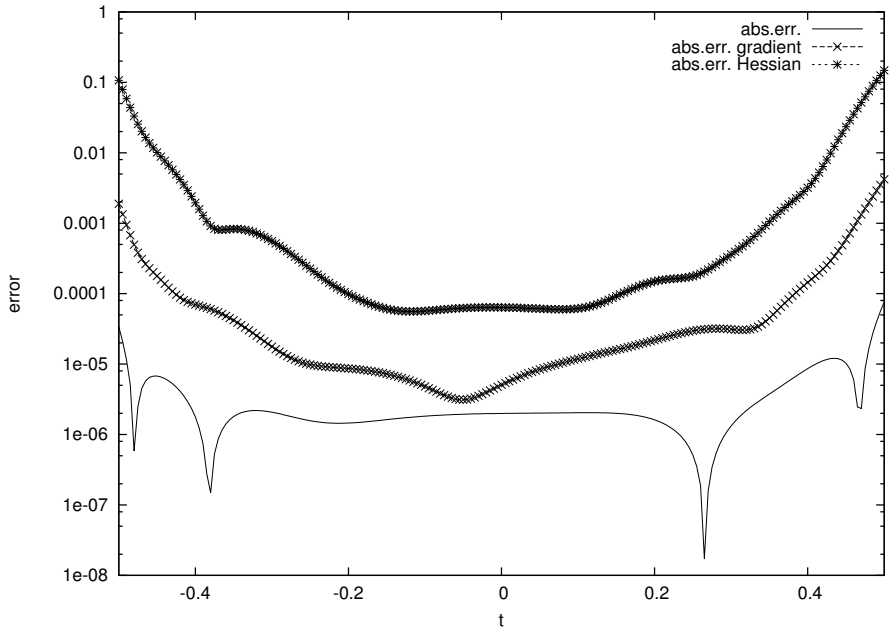

Figure 2: Absolute values of errors for Laplace problem on brick-shaped domain measured on a line segment. Downward spikes correspond to changes of sign.

Fundamental solutions as well as the derived basis functions of the adaptive method are $\mathcal{L}$-harmonic. Due to the maximum principle for Laplace equations the error assumes its maximum on the boundary of Ω. This can be illustrated in an error plot along the line segment $(t,t,t)^\top$, $t \in [-\frac{1}{2}, \frac{1}{2}]$, through the brick-shaped domain $[-2.5, 2.5] \times [-0.5, 0.5]^2$ (cf. Figure 2). The errors of the gradient and the Hessian show a similar behaviour.
Looking at the error on the boundary in case of the adaptive method one observes a pattern of low error speckles (cf. Figure 3). These correspond to collocation points where local errors have been eliminated. In this example the singularity points were located on an ellipsoidal pseudo boundary adapted to the domain's shape. One can observe a higher concentration of speckles in regions closer to the pseudo boundary. This is in agreement with the theory of classical FSM, where a lower distance between the boundaries leads to higher stability but slower convergence [6].

5.2 Helmholtz equation

We perform experiments for the Helmholtz equation

$$\begin{aligned} \Delta v(x) + \kappa^2 v(x) &= 0\,,\ \kappa = 2^n,\ n = 1, \ldots, 5 \quad \text{for } x \in \Omega\,, && (40) \\ v(x) &= g(x)\,, \quad \text{for } x \in \partial\Omega\,, && (41) \end{aligned}$$

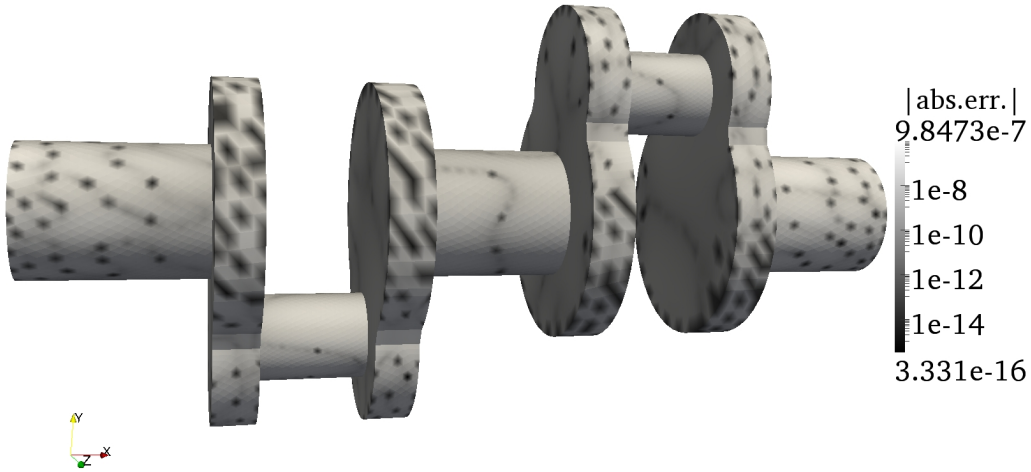

Figure 3: Absolute error for Laplace problem on the boundary of a crankshaft domain.

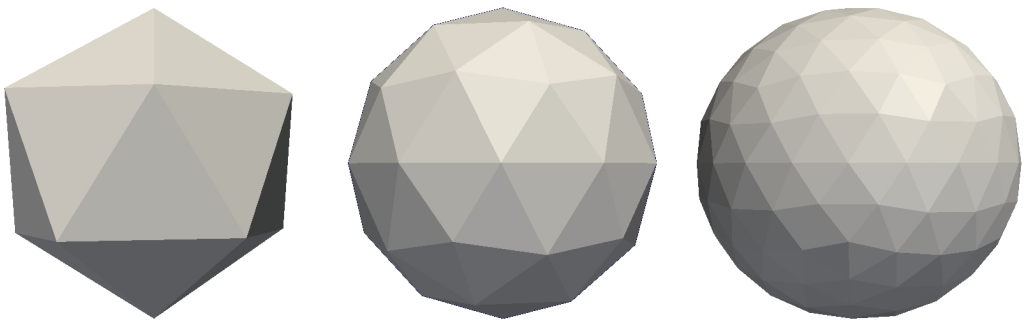

Figure 4: Approximations of unit sphere with 20, 80 and 320 triangles respectively.

κ	e (FSM)	e (aFSM, $\varepsilon = 10^{-11}$)	# nodes ($\varepsilon = 10^{-11}$)
1	$4.57 \cdot 10^{-13}$	$1.42 \cdot 10^{-11}$	976
2	$2.92 \cdot 10^{-13}$	$7.84 \cdot 10^{-12}$	1019
4	$6.46 \cdot 10^{-13}$	$6.18 \cdot 10^{-12}$	1102
8	$1.43 \cdot 10^{-12}$	$5.85 \cdot 10^{-12}$	1277
16	$3.00 \cdot 10^{-12}$	$5.94 \cdot 10^{-12}$	1792
32	$1.80 \cdot 10^{-11}$	$2.59 \cdot 10^{-11}$	3653 (no ε)

Table 2: Helmholtz equation, varying κ, $N = 20480$.

threshold	$e_{\max}$	e	cond_{sys}	cond_{LU}	# nodes
classical	$3.96 \cdot 10^{-10}$	$1.43 \cdot 10^{-10}$	$3.11 \cdot 10^{13}$	-	1280
10^{-8}	$1.20 \cdot 10^{-8}$	$7.40 \cdot 10^{-9}$	$8.36 \cdot 10^{2}$	$2.67 \cdot 10^{10}$	721
10^{-9}	$1.43 \cdot 10^{-9}$	$8.69 \cdot 10^{-10}$	$9.18 \cdot 10^{2}$	$2.73 \cdot 10^{11}$	872
10^{-10}	$5.39 \cdot 10^{-10}$	$1.86 \cdot 10^{-10}$	$1.01 \cdot 10^{3}$	$4.94 \cdot 10^{12}$	1042
10^{-11}	$3.94 \cdot 10^{-10}$	$1.47 \cdot 10^{-10}$	$1.08 \cdot 10^{3}$	$1.44 \cdot 10^{14}$	1200
10^{-12}	$3.96 \cdot 10^{-10}$	$1.43 \cdot 10^{-10}$	$1.11 \cdot 10^{3}$	$2.64 \cdot 10^{14}$	1276
10^{-13}	$3.96 \cdot 10^{-10}$	$1.43 \cdot 10^{-10}$	$1.12 \cdot 10^{3}$	$2.66 \cdot 10^{14}$	1278

Table 3: Helmholtz equation, $\kappa = 8$, $N = 1280$.

threshold	$e_{\max}$	e	cond_{sys}	cond_{LU}	# nodes
classical	$2.08 \cdot 10^{-12}$	$1.43 \cdot 10^{-12}$	$1.26 \cdot 10^{21}$	-	20480
10^{-10}	$9.86 \cdot 10^{-11}$	$6.06 \cdot 10^{-11}$	$3.13 \cdot 10^{3}$	$2.72 \cdot 10^{12}$	1086
10^{-11}	$1.01 \cdot 10^{-11}$	$5.85 \cdot 10^{-12}$	$3.43 \cdot 10^{3}$	$1.70 \cdot 10^{13}$	1277
10^{-12}	$1.02 \cdot 10^{-12}$	$6.15 \cdot 10^{-13}$	$3.65 \cdot 10^{3}$	$1.80 \cdot 10^{14}$	1493
10^{-13}	$1.08 \cdot 10^{-13}$	$5.97 \cdot 10^{-14}$	$3.98 \cdot 10^{3}$	$2.36 \cdot 10^{15}$	1753
none	$7.83 \cdot 10^{-14}$	$4.80 \cdot 10^{-14}$	$4.00 \cdot 10^{3}$	$3.99 \cdot 10^{15}$	1781

Table 4: Helmholtz equation, $\kappa = 8$, $N = 20480$.

with the known analytical solution

$$v(x) = \exp(-\frac{\kappa}{\sqrt{2}} i x_1) x_2 \sin(\frac{\kappa}{\sqrt{2}} x_3)\,, \quad g = v|_\Gamma.$$

Here Ω is the unit ball; its surface Γ is approximated by triangulated surface meshes. These meshes are obtained by quasi-uniform refinement starting from an icosahedron (cf. Figure 4). The collocation points are derived as barycenters of the mesh triangles, singularity points are obtained by shifting the collocation points along the surface normal. Although Fundamental Solution Methods do not require an actual mesh, we will stick to this term, since the collocation points are derived from meshes. In the examples presented here the distance between boundary and pseudo boundary is uniformly chosen as 1.

Performance of the adaptive FSM

As one would expect, for both, classical and adaptive FSM, the quality of results gets worse with increasing κ (cf. Table 2). While classical FSM suffers from a loss of approximation quality, the adaptive method compensates for this by use of a larger number of basis functions. For strict thresholds the adaptive method reaches the accuracy of the classical method on coarser meshes (cf. Table 3) and even outperforms it on fine meshes (cf. Table 4). On such meshes classical FSM suffers from extremely high condition numbers cond_{sys} of the system matrix leading to a loss of accuracy.

Number of required collocation points

An interesting observation is that, when increasing the number of available collocation points, the number of steps required in the adaptive method to reach a certain threshold does not seem to grow (cf. Figure 5). As can be seen in Table 5 on smaller clusters, where the threshold is reached faster, results are worse. This is due to the fact that on small clusters the lower number of available basis functions does not allow for the same level of accuracy, which is possible on larger clusters. Nevertheless, theoretically any threshold can be reached by eliminating all (or almost all) errors in the collocation points. In this case the adaptive method is equivalent to full FSM.

Effects of large condition numbers

Figure 6 shows the loss of accuracy in the classical Fundamental Solution Method. When the number of collocation points grows beyond a critical value, the error starts to grow slowly. While this growth does not neccessarily lead to very large errors, if a better approximation is desired, one has to repeat the calculation with fewer collocation points. In the same figure the growth of the condition number is indicated.

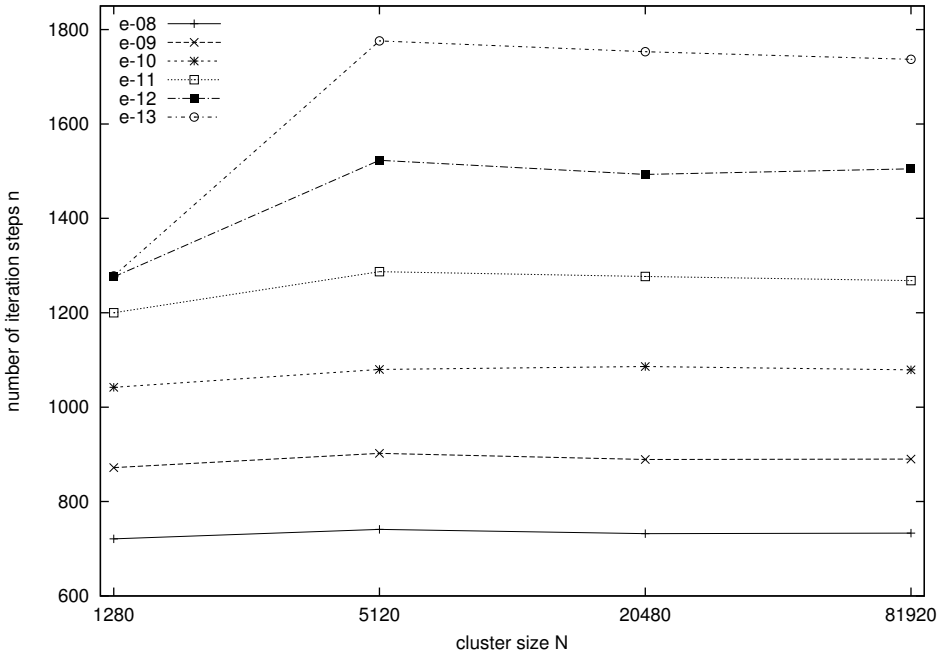

Figure 5: Number of iteration steps required to reach a certain threshold for a varying number of collocation points.

To the same problem the adaptive FSM is applied (cf. Figure 7). It can be seen that there exists a critical step after which the maximal local error will grow due to loss of accuracy in floating point operations. This loss leads to errors in the evaluation of basis functions, eventually causing the method to fail. However, we can still use stored data from the previous steps in order to obtain reasonable results. Note that the optimal step number is lower for the adaptive method than it is for classical FSM, while results are comparable. Thus it can be seen that adaptive FSM makes use of a more efficient basis than classical FSM with uniform refinement.

N	e (FSM)	e (aFSM)	# nodes
1280	$1.43 \cdot 10^{-10}$	$1.43 \cdot 10^{-10}$	1276
5120	$5.85 \cdot 10^{-13}$	$6.47 \cdot 10^{-13}$	1523
20480	$1.43 \cdot 10^{-12}$	$6.15 \cdot 10^{-13}$	1493
81920	-	$5.92 \cdot 10^{-13}$	1505

Table 5: Helmholtz equation, $\kappa = 8$, different geometries, threshold $\varepsilon = 10^{-12}$.

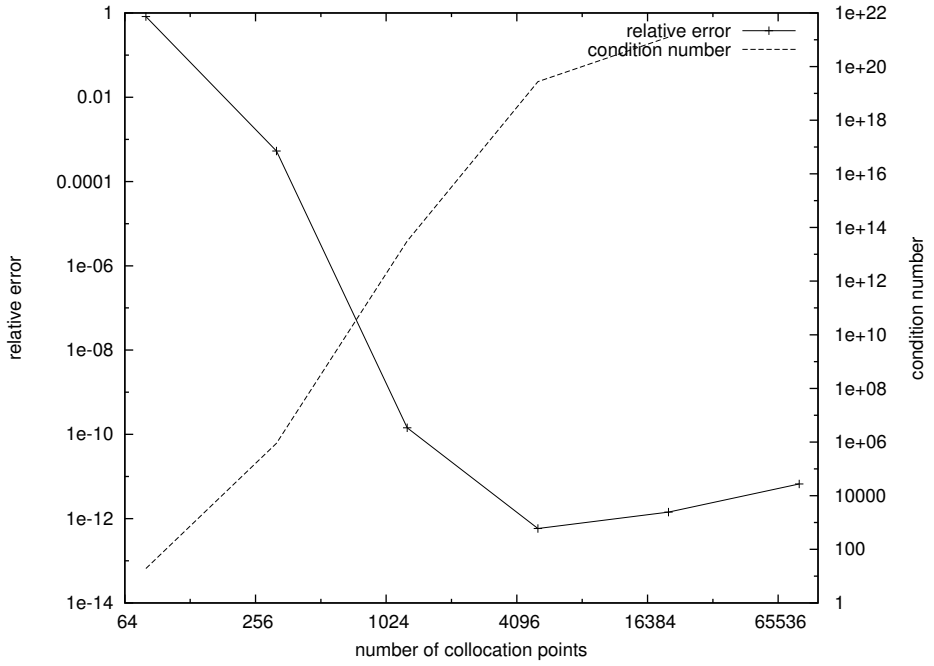

Figure 6: Full FSM: Condition number and loss of accuracy for large numbers of collocation points.

6 Conclusion and Outlook

When applied to large problems the Fundamental Solution Method features system matrices with extremely large condition numbers. We have presented an adaptive method where dimensions, and therefore also condition numbers, of the matrices involved are reduced by several orders. Numerical results show that the quality of approximations is comparable to that of the classical method. Also, the new method leads to reasonable results even in scenarios, where the classical method fails.

The present study shows, that the adaptive FSM can be used to find an approximation to the solution of the BVP (3) by means of a linear combination of basis functions (30,31) with a prescribed accuracy. If this prescribed accuracy is not achievable in the framework of the FSM (due to the high condition numbers and the finite errors of floating point operations), then the method returns the best approximation, which is attainable in the given settings.

Future work will include the extension of the adaptive method to vector-valued problems, with a special focus on elastostatics. We also plan to investigate the convergence of the method in a theoretical context.

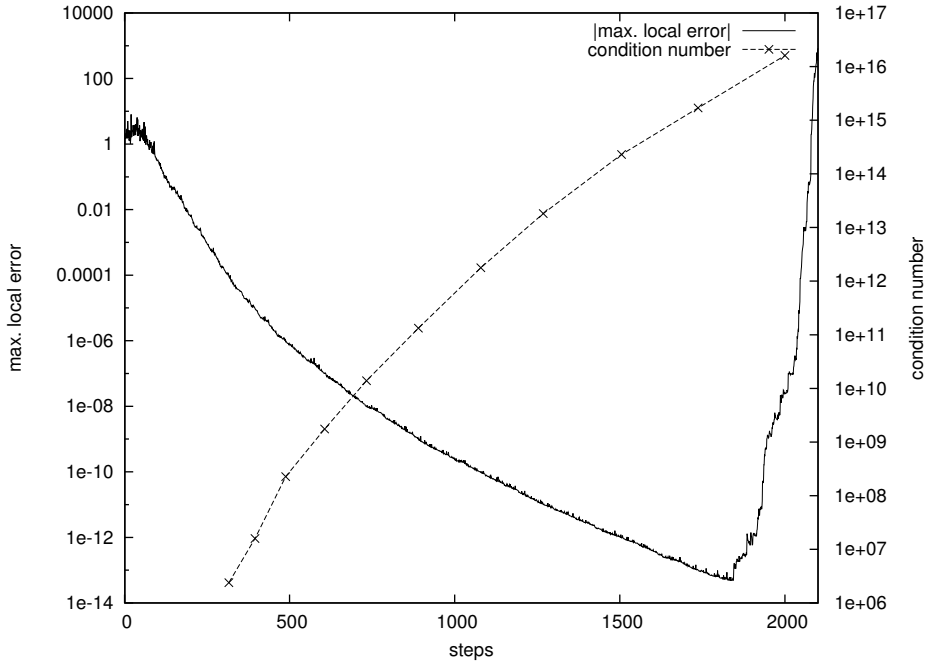

Figure 7: Adaptive FSM: Maximal local error, Helmholtz equation, $\kappa = 8$, $N = 81920$.

References

[1] E. Anderson, Z. Bai, C. Bischof, S. Blackford, J. Demmel, J. Dongarra, J. Du Croz, A. Greenbaum, S. Hammarling, A. McKenney, and D. Sorensen. *LAPACK Users' Guide*. Society for Industrial and Applied Mathematics, Philadelphia, PA, third edition, 1999.

[2] Mario Bebendorf. Approximation of boundary element matrices. *Numer. Math.*, 86(4):565–589, 2000.

[3] Alexander Bogomolny. Fundamental solutions method for elliptic boundary value problems. *SIAM J. Numer. Anal.*, 22(4):644–669, 1985.

[4] V. D. Kupradze and M. A. Aleksidze. An approximate method of solving certain boundary-value problems. *Soobšč. Akad. Nauk Gruzin. SSR*, 30:529–536, 1963.

[5] Rudolf Mathon and R. L. Johnston. The approximate solution of elliptic boundary-value problems by fundamental solutions. *SIAM J. Numer. Anal.*, 14(4):638–650, 1977.

[6] Yiorgos-Sokratis Smyrlis. Applicability and applications of the method of fundamental solutions. *Math. Comp.*, 78(267):1399–1434, 2009.

[7] E. Trefftz. Ein Gegenstück zum Ritzschen Verfahren. In *2ter Intern. Kongr. für Techn. Mech.*, pages 131–137, Zürich, 1926.